

I.
INTEGRATED INTENSITY MEASUREMENTS
FOR VIBRATION-ROTATION BANDS OF
CARBON DIOXIDE

II.
TOTAL ABSORPTIVITY MEASUREMENTS
ON CARBON DIOXIDE AT ROOM
TEMPERATURE

R. J. HOLM

THESIS
H69

Library
U. S. Naval Postgraduate School
Monterey, California

- I. INTEGRATED INTENSITY MEASUREMENTS FOR VIBRATION-
ROTATION BANDS OF CARBON DIOXIDE
- II. TOTAL ABSORPTIVITY MEASUREMENTS ON CARBON DIOXIDE
AT ROOM TEMPERATURE

Thesis by

Robert J. Holm

"

Lieutenant Colonel, United States Marine Corps

In Partial Fulfillment of the Requirements

For the Degree of

Aeronautical Engineer

California Institute of Technology

Pasadena, California

1952

Thos
H/29

ACKNOWLEDGMENTS

The author wishes to extend his appreciation to Dr. S. S. Penner, under whose direction this work was conducted, and to Mr. D. Weber for help with the experimental work.

ABSTRACT

I. This study contains an outline of the experimental measurements performed in order to determine integrated intensities of various vibration-rotation bands of carbon dioxide by use of standard techniques with a Perkin-Elmer spectrometer.

II. Total absorptivity measurements on carbon dioxide at room temperatures were made in a pressurized gas cell provided with transparent windows.

TABLE OF CONTENTS

Acknowledgements	i
Abstract	ii
Table of Contents	iii
Table of Figures	iv
Symbols	vi
I. Integrated Intensity Measurements on Carbon Dioxide	1
A. Introduction and Summary	1
B. Methods For the Experimental Determination of Integrated Intensities	2
C. Experimental Studies	6
D. Comparison With The Results of Other Investigators	7
E. Calibration of Perkin-Elmer Spectrometer with Sodium Chloride Prism	9
II. Total Absorptivity Measurements on Carbon Dioxide	
At Room Temperature	10
A. Introduction and Summary	10
B. Basic Radiation Laws	13
C. Total Absorptivity Determinations On Carbon Dioxide at Room Temperature	15
D. Comparison with the Results of Other Investigators	19

TABLE OF FIGURES

Figure	Title	Page
1.	Schematic Representation of Infrared Absorption Cell Used to Measure Intensities of Gas Mixtures	22
2.	$\beta/2.303$ as a function of p/l for the CO_2 band with center at 5109 cm^{-1} . $\alpha = .426 \pm .043 \text{ cm}^{-2} - \text{atm}^{-1}$ at 298°K . (3.57 cm cell length, $p_T = 90 \text{ psia}$)	23
3.	$\beta/2.303$ as a function of p/l for the CO_2 band with center at 4983 cm^{-1} . $\alpha = 1.01 \pm .10 \text{ cm}^{-2} - \text{atm}^{-1}$ at 298°K . (3.57 cm cell length, $p_T = 500 \text{ psia}$)	24
4.	$\beta/2.303$ as a function of p/l for the CO_2 band with center at 4860 cm^{-1} . $\alpha = .272 \pm .027 \text{ cm}^{-2} - \text{atm}^{-1}$ at 298°K . (3.57 cm cell length, $p_T = 500 \text{ psia}$)	25
5.	$\beta/2.303$ as a function of p/l for the CO_2 band with center at 3716 cm^{-1} . $\alpha = 42.3 \pm 4.23 \text{ cm}^{-2} - \text{atm}^{-1}$ at 298°K . (.5 cm cell length, $p_T = 500 \text{ psia}$)	26
6.	$\beta/2.303$ as a function of p/l for the CO_2 band with center at 3609 cm^{-1} . $\alpha = 28.50 \pm 2.85 \text{ cm}^{-2} - \text{atm}^{-1}$ at 298°K . (.5 cm cell length, $p_T = 500 \text{ psia}$)	27
7.	$\beta/2.303$ as a function of p/l for the CO_2 band with center at 3349 cm^{-1} . $\alpha = 2706 \pm 270 \text{ cm}^{-2} - \text{atm}^{-1}$ at 298°K . (5.15 cm cell length, $p_T = 700 \text{ psia}$)	28
8.	$\beta/2.303$ as a function of p/l for CO_2 in the region between 3000 and 2160 cm^{-1} . $\alpha = .147 \pm .047 \text{ cm}^{-2} - \text{atm}^{-1}$ at 298°K . (3.57 and 6.72 cm cell length, $p_T = 500 \text{ psia}$)	29
9.	$\beta/2.303$ as a function of p/l for CO_2 in the region between 1800 and 2000 cm^{-1} . $\alpha = .083 \pm .008 \text{ cm}^{-2} - \text{atm}^{-1}$ at 298°K . (6.72 cm cell length, $p_T = 400 \text{ psia}$)	30

TABLE OF FIGURES (Cont'd)

Figures	Title	Page
10.	$\beta/2.303$ as a function of pl for CO_2 band with center at 668 cm^{-1} including weak neighboring bands with centers at 720 , 667 and 618 cm^{-1} . $\alpha = 171.6 \pm 17.1 \text{ cm}^{-2} - \text{atm}^{-1}$ at 298°K . (1.985 cm cell length, $p_T = 500 \text{ psia}$)	31
11.	Calibration curve for infrared spectrometer with NaCl prism	32
12.	Calibration curve for infrared spectrometer with NaCl prism	33
13.	Block diagram of apparatus for measurement of total absorption of infrared radiation	34
14.	Absorptivity α as a function of p_T for various fractional pressures of CO_2 at room temperature. (The CO_2 was pressurized with nitrogen)	35
15.	Absorptivity α as a function of pl for CO_2 at room temperature and a total pressure of one atmosphere	36
16.	Absorptivity α as a function of pl for CO_2 at room temperature and a total pressure of one atmosphere	37
17.	Absorptivity α of CO_2 at room temperature as a function of pl at various total pressures	38
18.	Comparison of experimentally determined absorptivities as a function of optical density for CO_2 at atmospheric pressure and room temperature with the results of studies carried out by Hottel and Mangelsdorf	39
19.	Comparison of experimentally determined absorptivities as a function of optical density for CO_2 at atmospheric pressure and room temperature with the results of studies carried out by Hottel and Mangelsdorf	40

SYMBOLS

Part I

α	=	integrated intensity
P_{ω}	=	spectral absorption coefficient
ω	=	wave number
ν	=	quantum number
I_{ω}	=	transmitted intensity
$I_{0\omega}$	=	incident intensity
p	=	partial pressure
l	=	optical path length
$T_{0\omega}$	=	apparent intensity without absorber
T_{ω}	=	apparent intensity with absorber
α'	=	apparent integrated intensity
β	=	$p l / \alpha'$
P_T	=	total pressure
T	=	micrometer screw turns
B	=	defined spectrometer constant
ω_2	=	Reststrahlen wave number
$p l$	=	optical density

Part II

R_{λ}	=	energy emitted by a blackbody at temperature T at wave length λ
R_{ω}	=	energy emitted by a blackbody at temperature T at wave number ω

SYMBOLS (Cont'd)

λ	=	wave length
ω	=	wave number
c_1, c_2	=	physical constants
c	=	velocity of light
h	=	Planck's constant
k	=	Boltzmann's constant
T	=	absolute temperature
σ	=	Stephan Boltzmann constant
ϵ	=	emissivity
R_ω	=	spectral intensity of emission from greybody
ϵ	=	engineering emissivity
K	=	recorder constant
K'	=	defined recorder constant
D	=	recorder deflection
α	=	absorptivity
T_s	=	global temperature

I. INTEGRATED INTENSITY MEASUREMENTS ON CARBON DIOXIDE

A. Introduction and Summary

The importance of gas radiation in effecting heat transfer between a gas and its surroundings, particularly when the gas temperature is high, has been recognized for some time. However, accurate emissivity data are generally not available for use in engineering calculations of heat transfer. Recently attempts have been made to calculate gas emissivities theoretically from spectroscopic data. It is the purpose of the present study to provide some of the basic data which are needed for the theoretical calculation of emissivities of carbon dioxide.

Quantitative infrared intensity measurements have been carried out for the more intense vibration-rotation bands of carbon dioxide using helium as a pressurizing agent. Measurements were made by use of standard techniques. The results are summarized in Table I.

Table I. Observed Integrated Intensities* of Carbon Dioxide

Band Center (cm^{-1})	Integrated Intensity ($\text{cm}^{-2} \text{ atm}^{-1}$ at 298°K)	Band Center (cm^{-1})	Integrated Intensity ($\text{cm}^{-2} \text{ atm}^{-1}$ at 298°K)
5109	.43	1932	} combined .83
4983	1.01	1886	
4860	.27	720	} combined 171.50
3716	42.30	668	
3609	28.50	647	
2349	2706.00	612	
2137	} combined .147		
2094			
2074			

* Observed intensities are accurate within $\pm 20\%$.

B. Methods For the Experimental Determination of Integrated Intensities

Integrated intensities of the infrared vibration-rotation bands are required for the theoretical calculation of gas emissivities and radiant heat transfer.

The integrated intensity α for a given vibration-rotation band is defined by the relation

$$\alpha = \int P_{\omega} d\omega \quad (1)$$

where P_{ω} represents the spectral absorption coefficient at the wave number ω . Although the limits of integration should extend from $-\infty$ to $+\infty$ it is sufficient to restrict integration to a narrow wave number interval bracketing the band center because P_{ω} decreases very rapidly with ω in the wings of the vibration-rotation bands. The integrated intensities for various vibration-rotation bands will be identified by appropriate changes in vibrational quantum number. For example, the intense ν_3 - fundamental of carbon dioxide arises as a result of the transition*(2)

$$v_1 = 0 \rightarrow v_1 = 0, \quad v_2 = 0 \rightarrow v_2 = 0, \quad l = 0 \rightarrow l = 0, \quad v_3 = 0 \rightarrow v_3 = 1$$

and has a band center at 2349.3 cm^{-1} . The corresponding value of the integrated intensity is then identified by the symbol

* For details concerning spectroscopic notation of polyatomic molecules see, for example, G. Herzberg, Infrared and Raman Spectra, D. Van Nostrand Co., New York (1945).

$$\propto (0,0,0 \rightarrow 0,0,1)$$

The integrated intensities of other vibration-rotation bands may be identified similarly.

a) The Method of Wilson and Wells⁽²⁾

For monochromatic radiation it is well known that

$$I_{\omega} = I_{0\omega} \exp(-p_{\omega} p l) \quad (2)$$

where I_{ω} is the transmitted intensity at the wave number ω when the incident intensity is $I_{0\omega}$, p is the partial pressure of the absorbing gas and l represents the optical path length. Hence the integrated intensity becomes

$$\alpha = (p l)^{-1} \int_{\Delta \omega} \ln(I_{0\omega} / I_{\omega}) d\omega \quad (3)$$

where the integration in Eq. (3) is to be performed over the entire effective width $\Delta \omega$ of the vibration-rotation band under study.

The apparent intensities observed without absorber and with absorber, when the instrument is set at ω , are not $I_{0\omega}$ and I_{ω} respectively, but rather

$$T_{0\omega} = \int I_{0\omega'} g(\omega, \omega') d\omega' \quad (4)$$

and

$$T_{\omega} = \int I_{\omega'} g(\omega, \omega') d\omega' \quad (5)$$

where $g(\omega, \omega')$ represents the fraction of light of actual wave number ω' to which the instrument responds when it is set at ω . Some of the difficulties inherent in the calculation of P_ω do not arise in the determination of the integrated intensity. From experimentally determined values of T_ω and $T_0\omega$ it is possible to determine an apparent integrated intensity α' which is defined by the relation

$$\alpha' = (pl)^{-1} \int \ln(T_0\omega / T_\omega) d\omega = \beta/pl \quad (6)$$

Wilson and Wells⁽²⁾ have shown that

$$\lim_{pl \rightarrow 0} \alpha' = \alpha$$

when a number of specified conditions are met. These conditions include the requirement that $I_0\omega$ be independent of ω in the resolved spectral range, a condition which can be approached closely by eliminating atmospheric absorption and using sufficiently narrow spectrometer slits to give high spectral resolution. In addition to requiring constant $T_0\omega$, Eq. (6) will hold only if either the variation of P_ω with ω can be neglected in the spectral range or the resolution of the instrument does not vary appreciably over the vibration-rotation band under study. Of these two requirements the latter constitutes an intrinsic property of the instrument. The variation of P_ω in the resolved spectral interval can be minimized

by pressure broadening, i.e., as $p\ell$ is decreased, α' will approach α more rapidly, the higher the constant total pressure at which the observations are made.

As the optical density is decreased, the plot of β vs $p\ell$ may show considerable curvature. This fact introduces an appreciable error into the extrapolation required to determine α . At sufficiently high total pressure p_T , the variation of β with $p\ell$ should follow a linear relation in accord with the fact that the true integrated intensity is measured at every value of the optical density and Eq. (6) should apply directly. By proceeding according to Wilson and Wells⁽²⁾ the result $\alpha' \rightarrow \alpha$ as p_T is increased can be demonstrated.⁽³⁾

The true value of the integrated intensity α can be obtained either by extrapolating α' to zero values of $p\ell$ at constant p_T or by finding the limiting value of α' at constant optical density as the total pressure is increased.

b) The Self-Broadening Technique of Penner and Weber⁽⁴⁾

Infrared transmission studies on pure gases have the obvious advantage of eliminating the possibility of experimental error resulting from imperfect mixing or from the occurrence of adsorption-desorption phenomena. On the other hand, they possess the severe disadvantage of always involving the effect of significant self-broadening associated with increased pressure of the absorber. How-

ever, by suitable choice of test cell length it is possible to utilize self-broadening to obtain quantitative infrared intensity data. In general, the required cell length is shorter when the vibration-rotation band is more intense.

C. Experimental Studies

a) Apparatus

A Perkin-Elmer Model 125 single beam infrared spectrometer with lithium fluoride, sodium chloride, and potassium bromide prisms was used for transmission measurements. Incorporation of automatic slit drive over the wavelength interval used for study was found to save considerable time in experimental work. Pressure readings were performed by use of a Wallace and Tieman precision manometer for the pressure range 0-800 mm of mercury ($\pm .2$ mm) and 0-1000 psig by use of a Marsh gage (± 2 psig).

The cell and window assemblies were machined from 18-8 stainless steel stock. Neoprene O-rings and neoprene or teflon gaskets were used to support the cell windows. The principal features of the cell are shown in Fig. 1. The right end plate is provided with a special tap to permit flushing with nitrogen of the outside of the cell in the light path. This same end plate is fitted with a flange to slide into the absorption cell slot provided on the spectrometer. A flexible collar is inserted between the other end plate and the globar source. The collar also has a fitting for nitrogen flushing.

The cell is provided with a window assembly as shown and is large enough to permit incorporation of stirring rod with perforated end plate. In each experiment care was taken to assure uniform mixing of gases in the cell by adequate use of the stirrer. It was assumed that a uniform gas mixture had been obtained when additional stirring produced no measurable change in transmission.

Details of wavelength calibration of the prism spectrometer using a sodium chloride prism are given in Section E.

b) Summary of Experimental Data

For the vibration-rotation bands of carbon dioxide on which experimental measurements were performed the quantity $\beta / 2.303$ has been plotted as a function of $p \ell$ in Figs. 2 to 10. Corresponding integrated intensities have been given previously in Table I.

D. Comparison With The Results of Other Investigators

The observed intensities of vibration-rotation bands of carbon dioxide are compared with the results of other investigators in Table II. Reference to Table II shows that the data are in excellent agreement with the results of other investigators.

Table II. Observed Intensities of Carbon Dioxide

Integrated Intensity α ($\text{cm}^2 \text{ atm}^{-1}$ at 298°K)			
Band Center (cm^{-1})	Wilson et al 2,5,6 (1941)	Eggers and Crawford (7) + 10% (1951)	Present Study + 20% (1952)
5109			.426
4983			1.01
4860			.272
3716		39.0	42.3
3614		27.0	28.5
2349	2867.0	2693.0	2706.0
2137			
2094			
2074		0.14 (P and Q)	} combined .147
2074		.05 (Q only)	
1932		.005	} combined .083
1886			
720			
668	187.0	161.0	} combined 171.5
647			
618			

E. Calibration of Perkin-Elmer Spectrometer with Sodium Chloride Prism

In the wave number calibration of an infrared spectrometer it may become necessary to make use of the relation between micrometer screw turns and wave number in wave number regions where no calibration points (absorption bands or lines) exist or are available.

In the present calibration it was necessary to extrapolate the micrometer screw turns vs. wave number curve from the carbon dioxide band at 667 cm^{-1} to regions near the absorption limit of the sodium chloride prism. This was done using the method of McKinney and Friedel,⁽⁸⁾ whose empirical equation is

$$T = T_0 - B (\omega_2^2 - \omega^2)^{-1} \quad (7)$$

where T is micrometer screw turns and T_0 is the ordinate intercept at $B(\omega_2^2 - \omega^2)^{-1} = 0$. Here ω_2 is the Reststrahlen wave number depending on the prism material and ω is a known or measured wave number. Seven absorption maxima of ammonia and carbon dioxide were used for calibration and $(\omega_2^2 - \omega^2)^{-1}$ was calculated and plotted against micrometer screw turns. For sodium chloride the value of ω_2 is 125 cm^{-1} .

The constants T_0 and B are determined from the known absorption maxima. Equation (7) is used to extend the calibration curve of T vs ω . The correction term for short wave length absorption was neglected for the present purpose. Figures 11 and 12 are reproductions

of original calibration graphs in which the abscissae are, respectively, ω and $(\omega_2^2 - \omega^2)^{-1}$, whereas each ordinate represents micrometer screw turns.

II. TOTAL ABSORPTIVITY MEASUREMENTS ON CARBON DIOXIDE AT ROOM TEMPERATURE

A. Introduction and Summary

The calculation of radiant heat transfer from heated carbon dioxide requires the use of experimentally determined absorptivity data. The total absorption of radiation by carbon dioxide has been reinvestigated at various optical densities at different total pressures and at room temperature. A complete investigation could not be carried out at other temperatures because of experimental difficulties with the gas cell and amplifying system. The measured values of the total absorptivities are given in Table III.

Table III. Absorptivity α of Carbon Dioxide at Room Temperature and Different Total Pressures
(p_l refers to optical density of carbon dioxide).

P_T (atm)	$P_{CO_2}/P_T = .012$ p_l α (ft atm)	$P_{CO_2}/P_T = .0596$ p_l α (ft atm)	$P_{CO_2}/P_T = .1560$ p_l α (ft atm)	$P_{CO_2}/P_T = .2705$ p_l α (ft atm)	$P_{CO_2}/P_T = .5177$ p_l α (ft atm)	$P_{CO_2}/P_T = 1$ p_l α (ft atm)		
1	.00226	.015	.024	.038	.0510	.041	.189	.061
2.36	.00324	.023	.026	.053	.1205	.056	.445	.084
3.72	.00341	.027	.039	.063	.190	.070	.702	.095
5.08	.0115	.030	-	.066	.259	.079	.959	.103
7.80	.0176	.035	.052	.076	.380	.080	1.47	.114
14.60	.0213	.043	.062	.086	.745	.094	2.76	.133
21.41	.0485	.048	.070	.090	1.093	.102	4.04	.146
35.01							6.60	.180
48.62							9.17	.214
55.42							10.45	.225

B. Basic Radiation Laws

The spectral distribution of radiation from a blackbody is given by Planck's radiation law⁽⁹⁾

$$R_{\lambda} d\lambda = c_1 \lambda^{-5} \left[\exp (c_2/\lambda T) - 1 \right]^{-1} d\lambda \quad (7)$$

where $R_{\lambda} d\lambda$ is the energy emitted from a blackbody at temperature T per unit time per unit area in the wave length interval from λ to λ plus $d\lambda$ throughout a solid angle 2π steradians. c_1 and c_2 are physical constants whose values are given below: (10)

$$c_1 = 2 \pi c h^2 = (3.732 \pm .006) \times 10^{-5} \text{ erg cm}^2 \text{ sec};$$

$$c_2 = ch/k = (1.436 \pm .001) \text{ cm}^{\circ}\text{K};$$

$$c = \text{velocity of light} = (2.99776 \pm .00020) \times 10^{-10} \text{ cm sec}^{-1};$$

$$h = \text{Planck's constant} = 6.62 \times 10^{-27} \text{ erg sec};$$

$$k = \text{Boltzmann's constant} = 1.381 \times 10^{-16} \text{ ergs per molecule } ^{\circ}\text{K}^{-1}.$$

Equation (7) may be expressed in terms of wave number $\omega (= \lambda^{-1})$,

$$R_{\omega} d\omega = c_1 \omega^3 \left[\exp (c_2 \omega/T) - 1 \right]^{-1} d\omega \quad (8)$$

where $R_{\omega} d\omega$ is the energy emitted from a blackbody at temperature T per unit time per unit area in the wave number interval from ω to ω plus $d\omega$ throughout a solid angle 2π steradians.

The total intensity of radiation emitted by a blackbody over all wave lengths is given by Stephan's law

$$\int_0^{\infty} R_{\omega} d\omega = \sigma T^4 \quad (9)$$

where σ represents the Stephan-Boltzmann constant and has the numerical value⁽¹⁰⁾ $(5.67283 \pm .0037) \times 10^{-5} \text{ erg cm}^{-2} \text{ } ^\circ\text{K}^{-4} \text{ sec}^{-1}$ ($= 2\pi^5 k^4 / 15c^2 h^2$). For a greybody the emissivity ϵ is independent of wave number, i.e.,

$$R_{\omega}' = \epsilon R_{\omega} \quad (10)$$

where R_{ω}' is the spectral intensity of radiation emitted from a greybody. The engineering emissivity or absorptivity for diatomic and polyatomic gases is defined by a relation similar to Eq. (9). Thus, if I_{ω} is the spectrally emitted intensity from a non-black and a non-grey source, then the engineering emissivity E is given by

$$E = \int_0^{\infty} (I_{\omega} / \sigma T^4) d\omega \quad (11)$$

where I_{ω} is $R_{\omega} [1 - \exp(-P_{\omega} p\ell)]$, P_{ω} is the spectral absorption coefficient and $p\ell$ is the optical path density.

Equation (11) can be written more explicitly as a sum over the contributions to the total emissivity from separate vibration-rotation bands. Thus, let

$\Delta\omega' = \Delta\omega (v_1, v_2, v_3 \rightarrow v_1', v_2', v_3')$ represent the effective

width of the vibration-rotation band arising from the transition

$v_1, v_2, v_3 \xrightarrow{l, l'} v_1', v_2', v_3'$. Then

$$R = (\sigma T^4)^{-1} \sum_{v_1} \sum_{v_2} \sum_{l} \sum_{v_3} \sum_{v_1' \frac{1}{2} v_1} \sum_{v_2' \frac{1}{2} v_2} \sum_{l' \frac{1}{2} l} \sum_{v_3' \frac{1}{2} v_3} \int_{\Delta\omega} R_{\omega} [1 - \exp(-P_{\omega} p l)] d\omega \quad (13)$$

where the quantum numbers must conform to the selection rules for all allowed vibrational transitions. Quantitative calculations of R are exceedingly difficult to carry out.

C. Total Absorptivity Determinations on Carbon Dioxide at Room Temperature

An apparatus has been built for the measurement of absorptivity and emissivity of carbon dioxide. The system consists of a source of infrared radiation, a gas cell in which temperature and pressure may be controlled and a non-selective receiver. The signal from the receiver or detector is amplified using chopped radiation for stabilization. The percentage of transmission is found by comparing voltage output from the detector for an empty cell with voltage output from the detector for the same cell under test conditions. A recording potentiometer (Speedomax) is used to indicate voltage. A block diagram of the apparatus used for study of absorption and emission is shown in Fig. 13.

The source of radiation used is a globar unit which has a continuous emission spectrum in the infrared region.

The globar temperature must be held within close limits to reduce fluctuations in radiation. Power supply to the globar is regulated by a Sola constant voltage transformer.

The globar, gas cell, and detecting thermocouple are placed in a wooden chamber which is flushed with nitrogen to prevent light absorption by atmospheric water and carbon dioxide. The cell is fitted with potassium chloride windows which allow transmission at wave lengths longer than 20 microns.

The detector is a thermocouple which develops a signal of 100 microvolts with full globar input. Sensitivity of the thermocouple is specified as six microvolts per microwatt of incident radiation. This thermocouple is of the same type as that used in the Perkin-Elmer Model 12C Spectrometer and is reported to be linear in output over wide variations in light intensity at all wavelengths in the near infrared region. The thermocouple is sensitive to ambient temperature changes. Drift and instability produced by such changes are avoided by chopping incoming radiation at 13 cycles per second. Thus a low frequency A.C. amplifier may be used to amplify the very low level signal from the thermocouple. The A.C. signal is later rectified and filtered to recover information regarding signal amplitude. Contacts for the synchronous rectifier are operated by means of cams on the shaft of the synchronous motor used for the rotating shutter.

Emissivity as well as absorptivity may be measured with this system. For emissivity measurements it is only necessary to place the light chopper disk between the sample and the thermocouple rather than between the globar and the gas sample.

Since percentage of transmission is measured by noting the difference in radiation intensity received when the cell is evacuated and the radiation received when the cell contains gas at known temperature and pressure, it is important that measurements be made within the limits of linearity of the detecting and amplifying system. There is no easy means available for the measurement of absolute radiation intensity received at the thermocouple. The amplifier and Speedomax were found to be linear with respect to input signals from the detector.

Percentage of absorption by carbon dioxide at the temperature and pressure used was found to be of the order of 25% or less. In order to get reliable data it is necessary that noise and drift be low in comparison with variations in signal strength arising from changes in absorption of radiation. Noise and drift in the instrument were reduced to below the 1% level.

Previous investigations⁽¹⁰⁾ were carried out at a total pressure of one atmosphere while varying the partial pressure of the absorbing or radiating gas. We have investigated absorption of radiation at room temperature at total pressures up to 55 atmospheres.

Let D = recorder deflection for the filled gas cell and D_1 = the deflection for the empty cell, K = recorder constant, T_s = global temperature, ϵ_s = emissivity of source, σ = Stephan-Boltzmann constant, α = absorptivity and $K' = K/\sigma$. Then

$$KD_1 = \sigma \epsilon_s T_{s1}^4 \quad (14)$$

and, if $\epsilon_s = 1$,

$$K' = T_{s1}^4 / D_1 \quad (15)$$

When the gas cell contains absorbing gas and $\epsilon_s = 1$, then

$$K'D = (1-\alpha)T_{s1}^4 \quad (16)$$

$$\alpha = (T_{s1}^4 - K'D) / T_{s1}^4 \quad (17)$$

$$\alpha = 1 - D/D_1 \quad (18)$$

It follows from Kirchoff's law that the total absorptivity and emissivity of the carbon dioxide are equal to each other at equilibrium. At room temperature it has been assumed that the emission of radiation from carbon dioxide is negligibly small compared with the intensity of the transmitted incident radiation. The results of total absorption measurements are presented in Tables III and IV and are plotted in Figs. 14 to 17. Table III and Fig. 14 contain a summary of the experimental data which were actually

obtained. Table IV and Figs. 15 and 16 contain results applicable to a total pressure of 1 atmosphere. In Fig. 17 the absorptivity is plotted as a function of optical density with the total pressure p_T treated as a variable parameter. Reference to Fig. 17 shows that α is not a sensitive function of the total pressure at pressures in excess of about 3.73 atm.

Table IV. Absorptivity of Carbon Dioxide at a Pressure of 1 atm and at Room Temperature

$P l$ (ft-atm)	Absorptivity α	$P l$ (ft-atm)	Absorptivity α
10	.221	.4	.081
8	.197	.3	.064
6	.172	.1	.054
4	.148	.08	.050
3	.122	.06	.045
1.5	.113	.04	.039
1.0	.103	.03	.030
.8	.098	.01	.023
.6	.092		

D. Comparison with the Results of Other Investigators

The experimentally determined values of α at a total pressure of 1 atm are compared with the results of studies carried out by Hottel and Mangelsdorf⁽¹¹⁾ in Table V and in Figs. 18 and 19.

Since the limit of our probable error is $\pm 10\%$ and those of Hottel and Mangelsdorf $\pm 20\%$, the agreement between the independently determined experimental data may be considered to be satisfactory.

Table V. Absorptivity of Carbon Dioxide at Room Temperature at a Total Pressure of 1 Atmosphere.

p ℓ (ft atm)	Hottel and Mangelsdorf (1935)	Absorptivity α	Present Study
10			.221
8			.197
6			.172
4	.17		.148
2	.15		.122
1.5	.14		.113
1.0	.128		.103
.8	.120		.098
.6	.111		.092
.4	.100		.081
.2	.083		.067
.1	.068		.054
.08	.064		.050
.06	.057		.045
.04	.050		.039
.02	.038		.030
.01	.0285		.022
.008	.0252		
.006	.0219		
.004	.017		

REFERENCES

1. G. Herzberg, "Infrared and Raman Spectra, D. Van Nostrand Co., New York (1945).
2. E. B. Wilson, Jr. and A. J. Wells, J. Chem. Phys., 14, 578 (1946).
3. S. S. Penner and D. Weber, J. Chem. Phys., 19, 807-816 (1951).
4. S. S. Penner and D. Weber, J. Chem. Phys., 19, 817-818 (1951).
5. A. M. Thorndike, A. J. Wells, and E. B. Wilson, Jr., J. Chem. Phys. 15, 157 (1947).
6. A. M. Thorndike, J. Chem. Phys. 15, 868 (1947).
7. D. F. Eggers Jr. and B. L. Crawford, J. Chem. Phys., 19, 1556 (1951).
8. D. S. McKinney and R. A. Friedel, J. Opt. Soc. Am. 38, 222-225 (1948).
9. L. Page, Introduction to Theoretical Physics., D. Van Nostrand Co., New York (1935).
10. A. N. Lowan et al, "Miscellaneous Physical Tables", WPA Project No. 65-2-97-33. (1941).
11. M. Schmidt, Forsch. Geb. Ingen. 3, 57 (1932).
H. C. Hottel and H. G. Mangelsdorf, Trans. A.I.Chem. Engineering, 31, 517 (1935).
H. C. Hottel and V. C. Smith, Trans. A.S.M.E., 57, 4 (1935).
H. C. Hottel and R. B. Egbert, Trans. A.S.M.E., 63, 297 (1941).
R. B. Egbert, Sc. D., Thesis in Chemical Engineering, M.I.T. (1941).

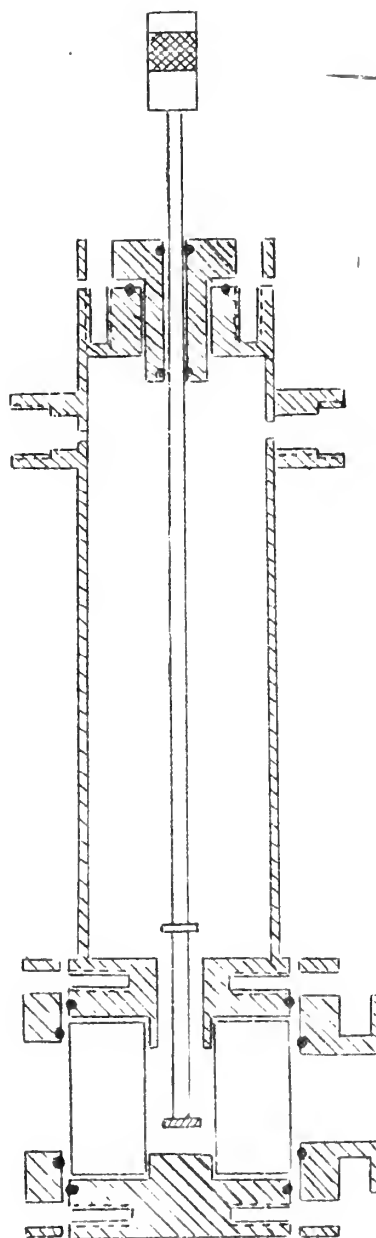


Fig. 1. Schematic representation of infrared absorption cell used to measure intensities of gas mixtures.

Fig. 2. $\beta/2.303$ as a function of p_l for the CO_2 band with center at 5109 cm^{-1} . $\alpha = .426 \pm .043 \text{ cm}^{-2} - \text{atm}^{-1}$ at 298°K .
(3.57 cm cell length, $p_T = 90 \text{ psia}$)

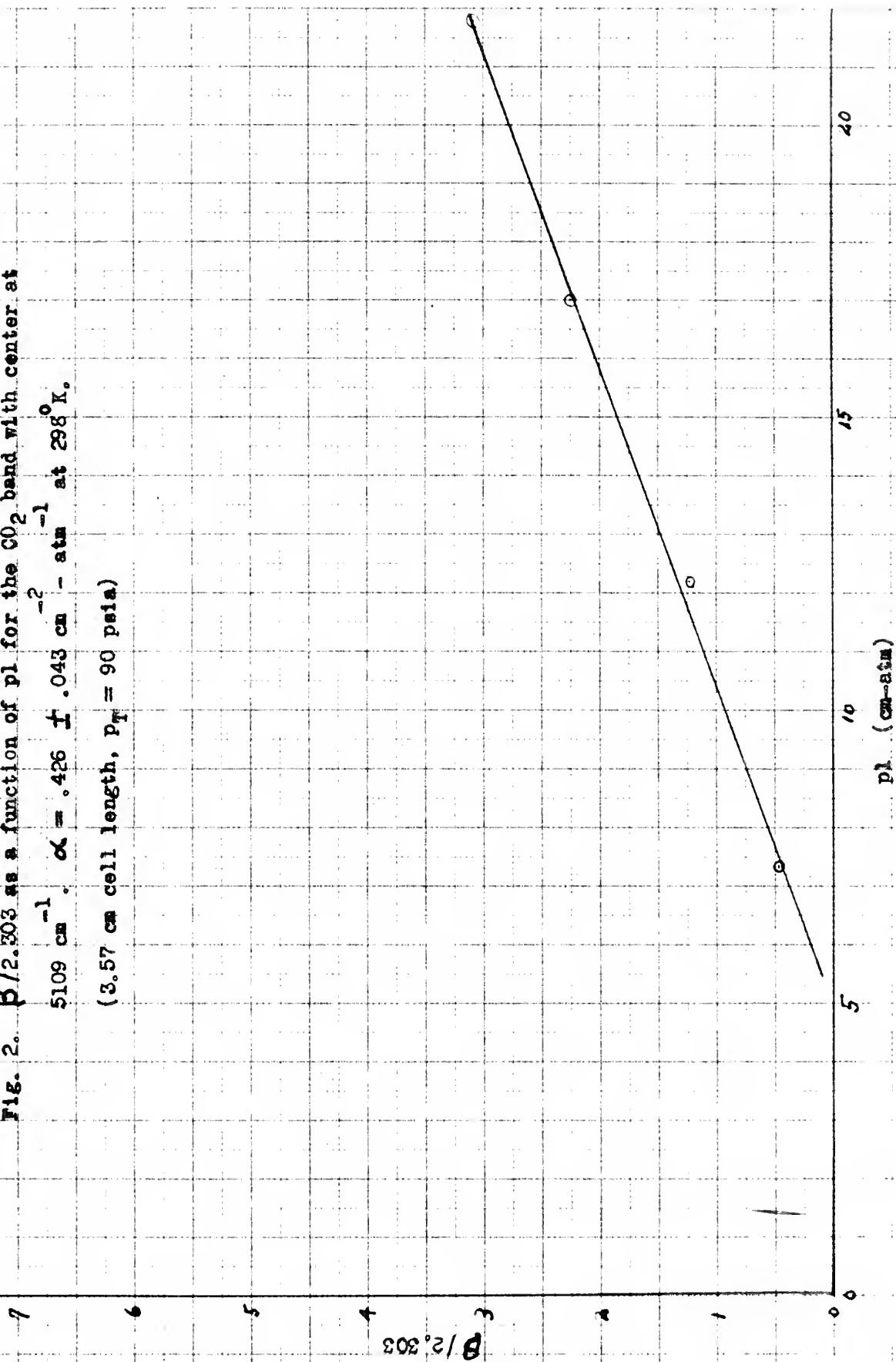


Fig. 3. $\beta/2.303$ as a function of pl for the CO_2 band with center at 4983 cm^{-1} . $\alpha = 1.01 \pm .10\text{ cm}^{-2}\text{ - atm}^{-1}$ at 298°K . (3.57 cm cell length, $p_T = 500\text{ psia}$)

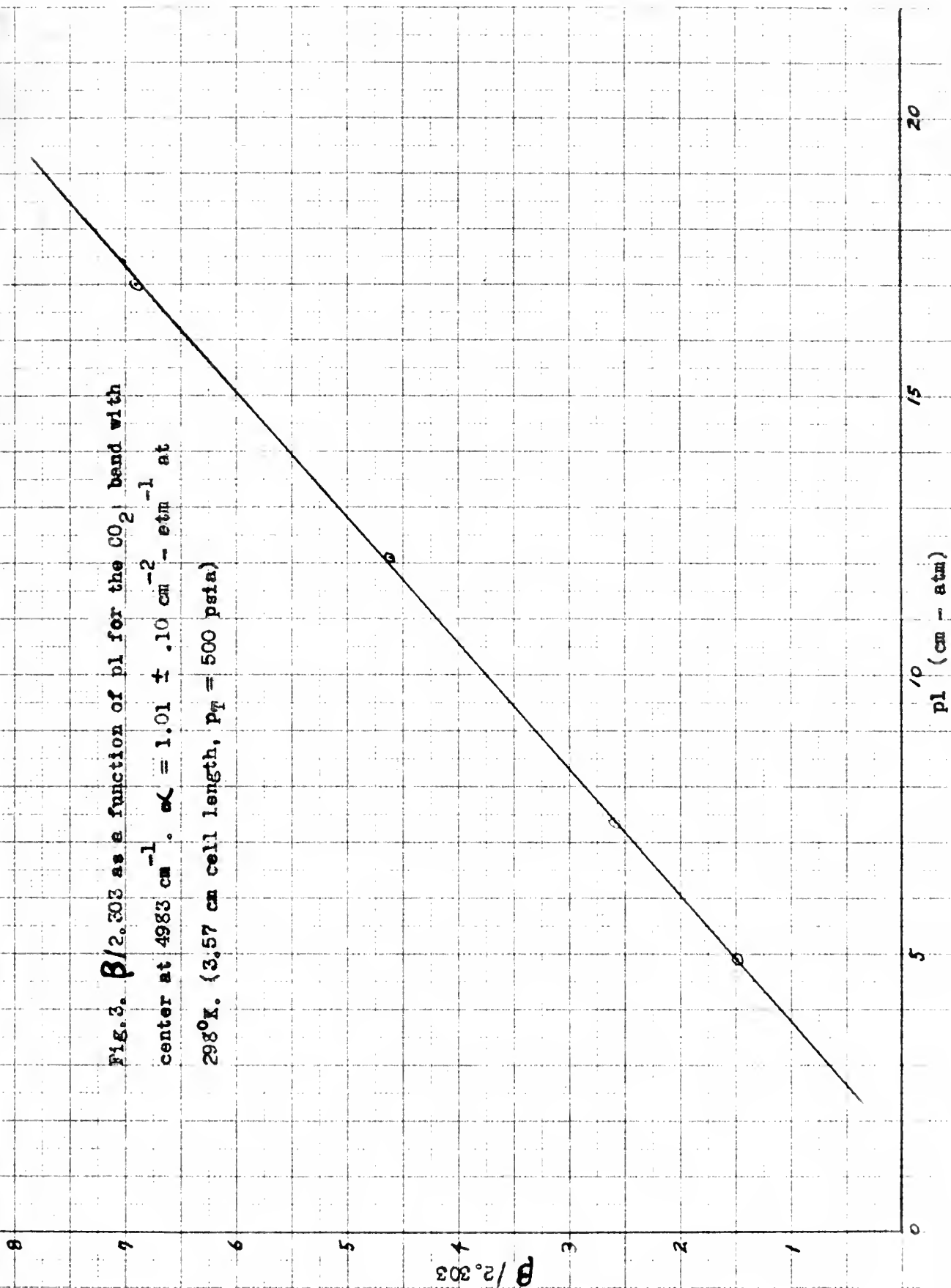


Fig. 4. $\beta/2.303$ as a function of p_l for the CO_2 band with center at 4860 cm^{-1} . $\alpha = .272 \pm .027 \text{ cm}^{-2} \text{ atm}^{-1}$ at 298°K .
(3.57 cm cell length, $p_T = 500 \text{ psia}$)

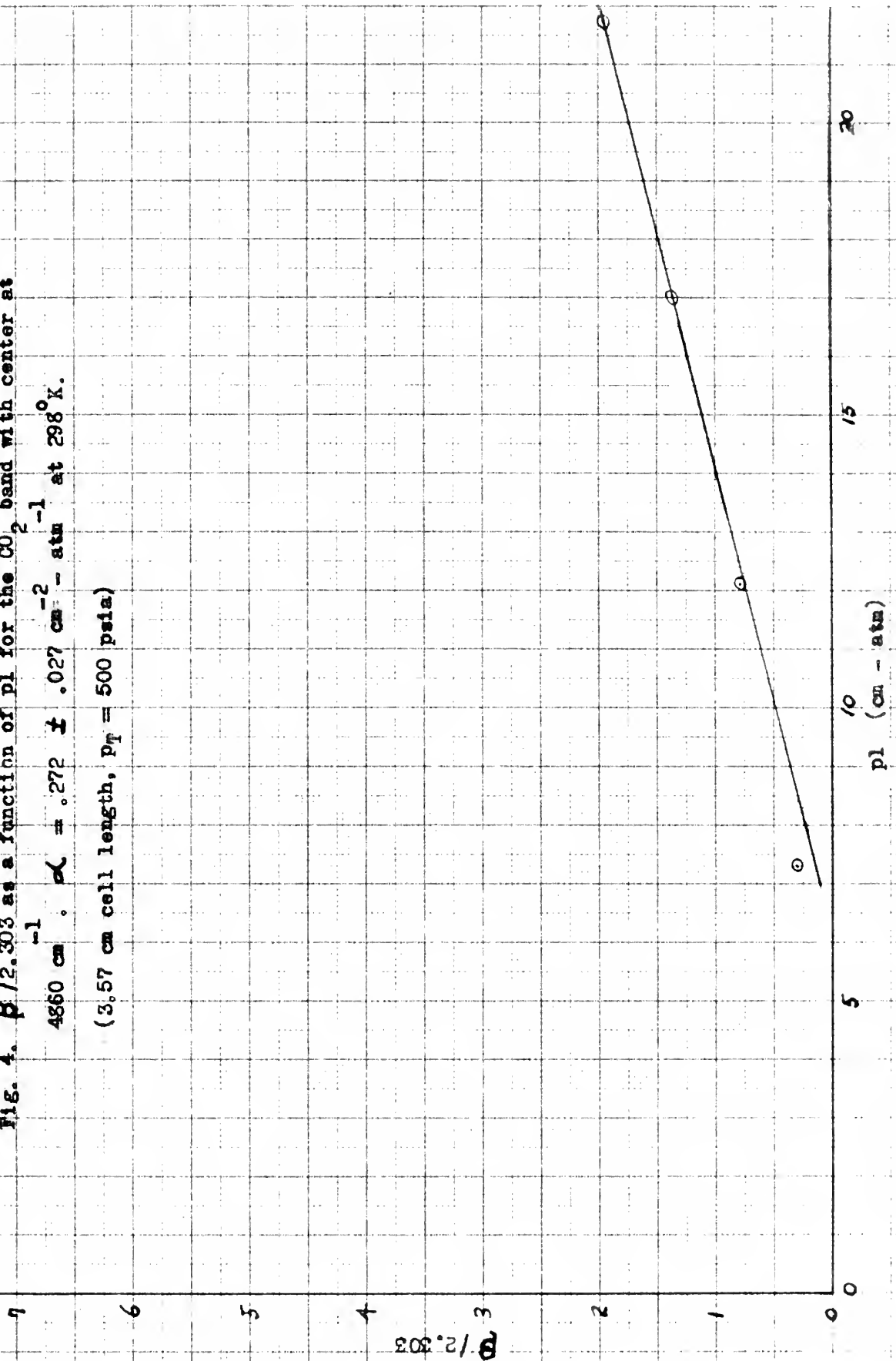


Fig. 5. $\beta/2.303$ as a function of p_l for the CO_2 band with center at 3716 cm^{-1} . $\alpha = 42.3 \text{ l} \cdot \text{atm}^{-2}$ at 298 K .
(.5 cm cell length, $p_T = 500 \text{ psia}$)

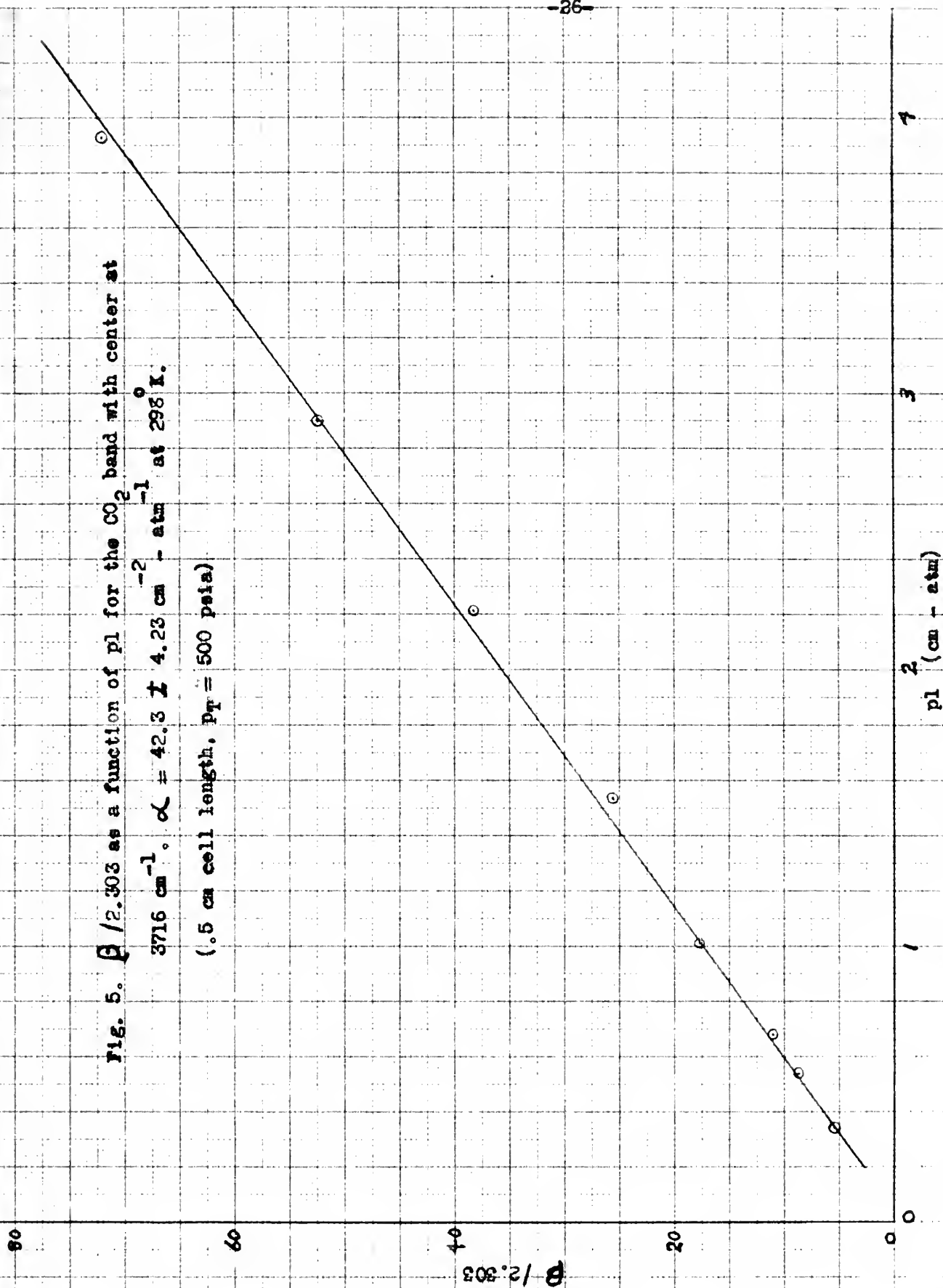


Fig. 6. $\theta/2.303$ as a function of p_l for the CO_2 band with center at 3609 cm^{-1} . $\alpha = 28.50 \pm 2.85 \text{ cm}^{-2} \cdot \text{atm}^{-1}$ at 298°K .
(.5 cm cell length, $p_T = 500 \text{ psia}$)

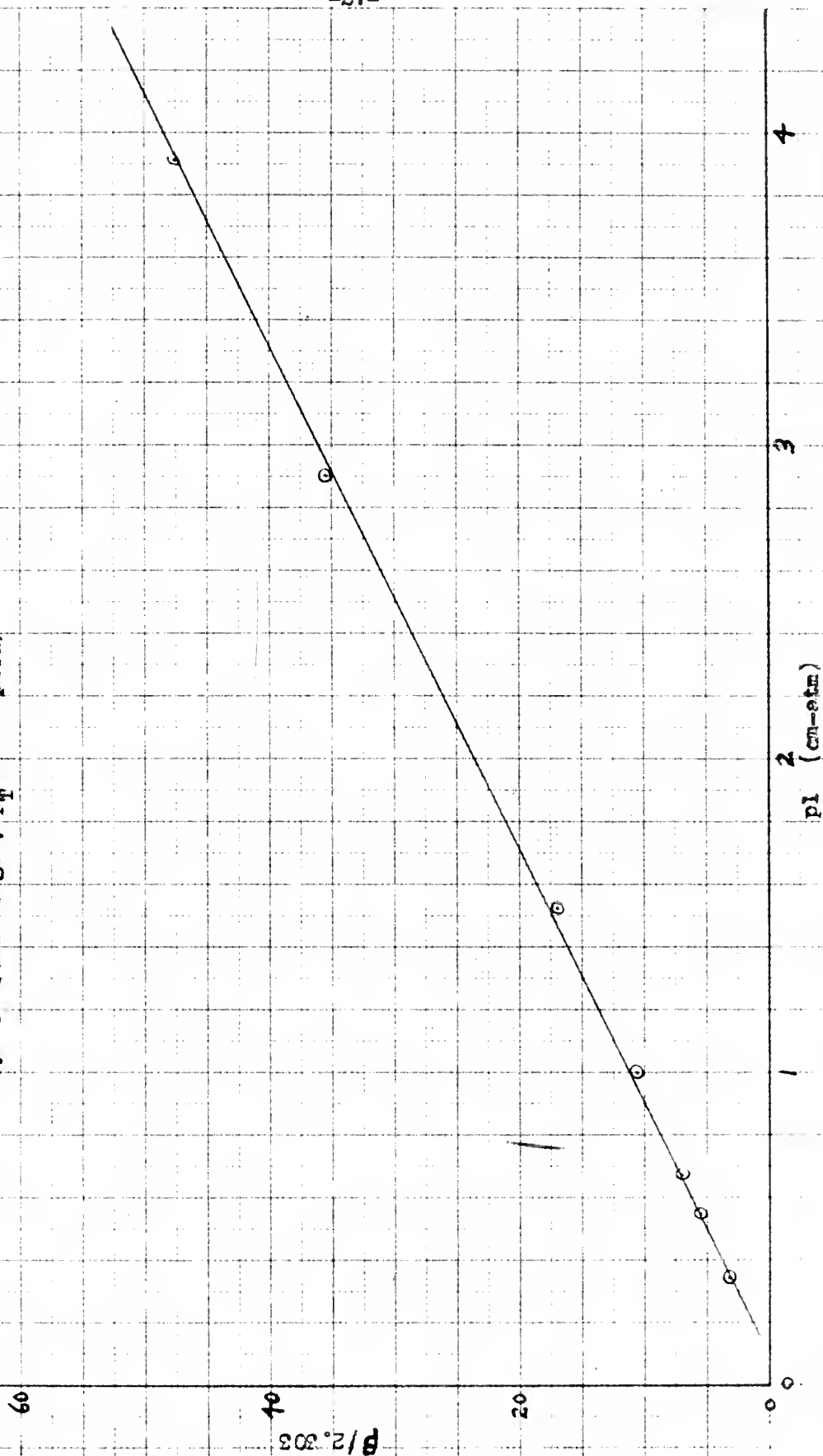


Fig. 7. $B / 2305$ as a function of pl for the CO_2 band with center at

2349 cm^{-1} . $\alpha = 2706 \pm 270 \text{ cm}^{-2} \cdot \text{atm}^{-1}$ at 298°K .

(5.15 cm cell length, $P_T = 700 \text{ psia}$)

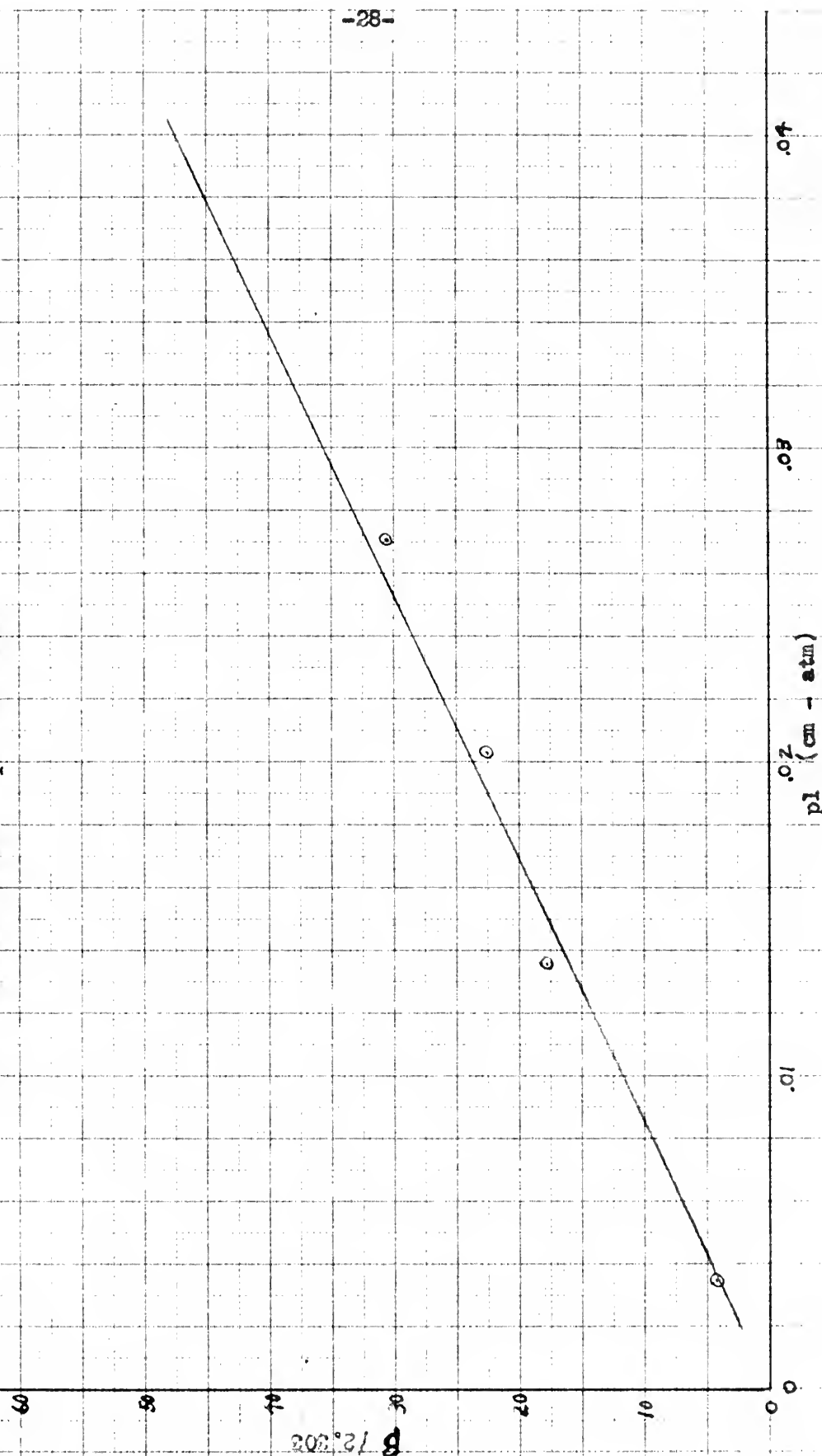


Fig. 8. $\beta / 2.303$ as a function of pl for CO_2 in the region between 2000 and 2160 cm^{-1} . $\alpha = .147 \pm .047 \text{ cm}^{-2} \text{ atm}^{-1}$ at 298°K .
(3.57 and 6.72 cm cell length, $p_T = 500 \text{ psia}$)

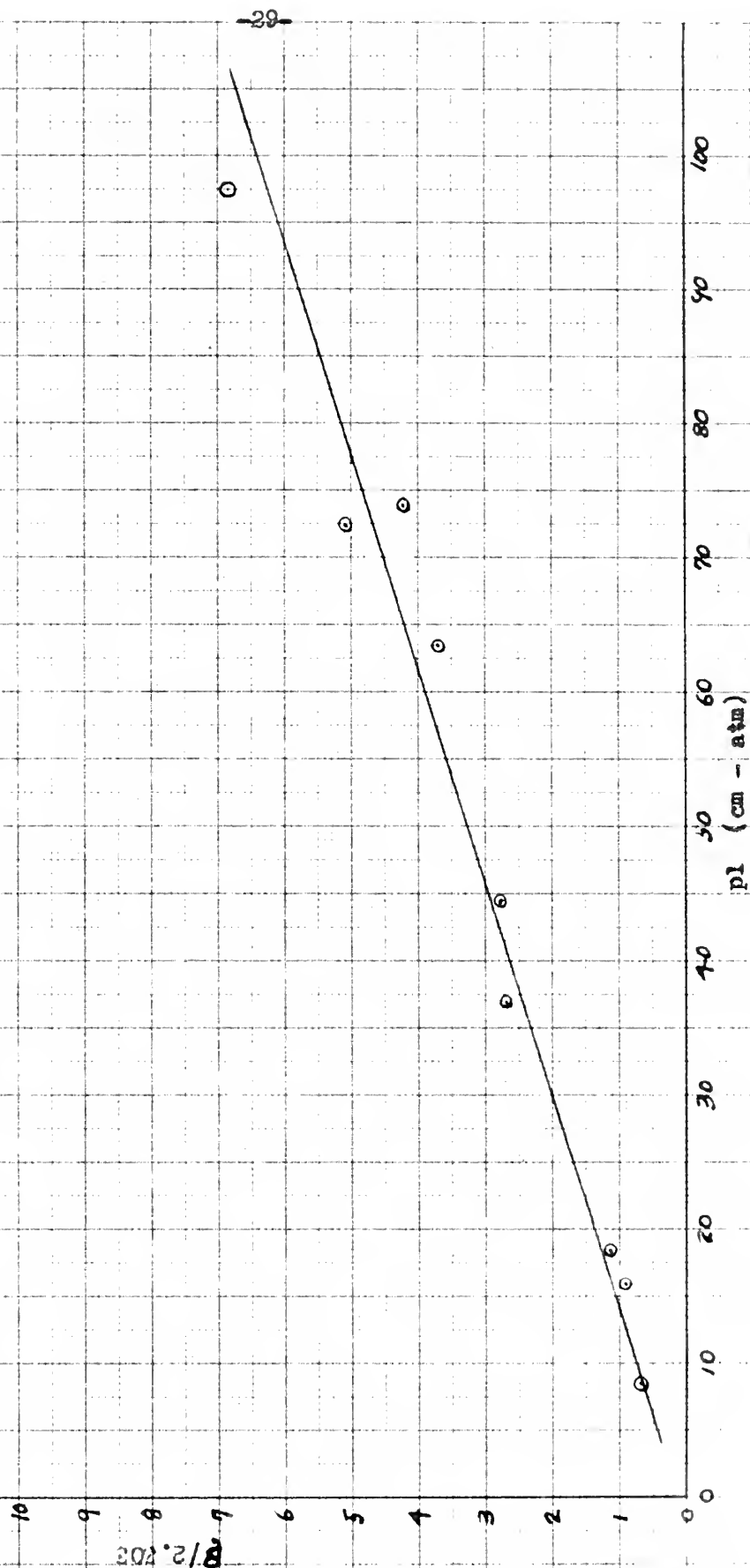


Fig. 9. $\beta/2.303$ as a function of pl for CO_2 in the region between 1800 and 2000 cm^{-1} . $\alpha = .083 \pm .008 \text{ cm}^{-2} - \text{atm}^{-1}$ at 298°K.
(6.72 cm cell length, $p_T = 400 \text{ psia}$)

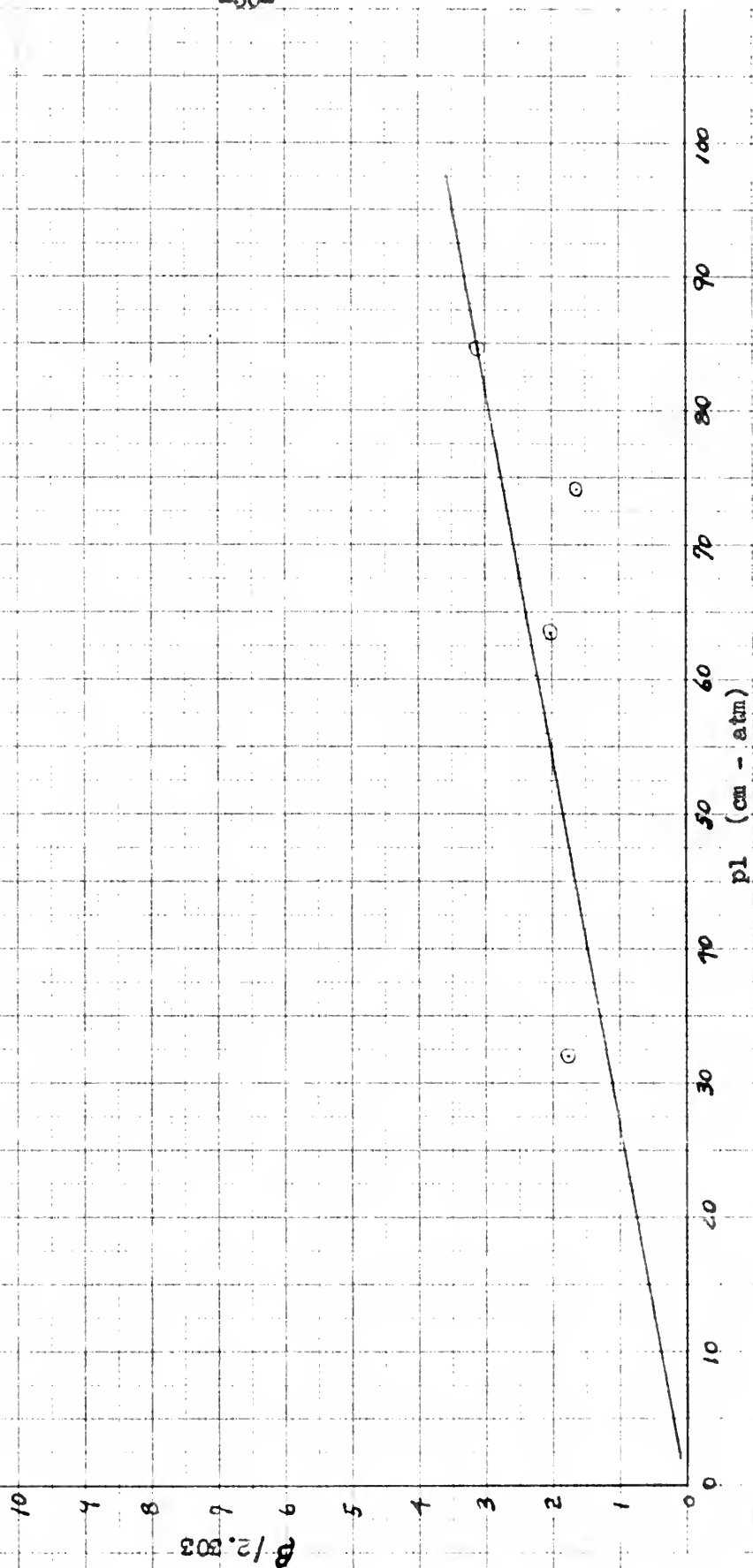


Fig. 10. $\beta / 2.303$ as a function of pl for the CO_2 band with center at 668 cm^{-1} including weak neighboring bands with centers at $720, 667$ and 618 cm^{-1} .

$$\alpha = 171.5 \pm 17.1\text{ cm}^{-2}\text{ atm}^{-1}\text{ at }298^\circ\text{K}.$$

(1.985 cm cell length, $p_T = 500\text{ psia}$)

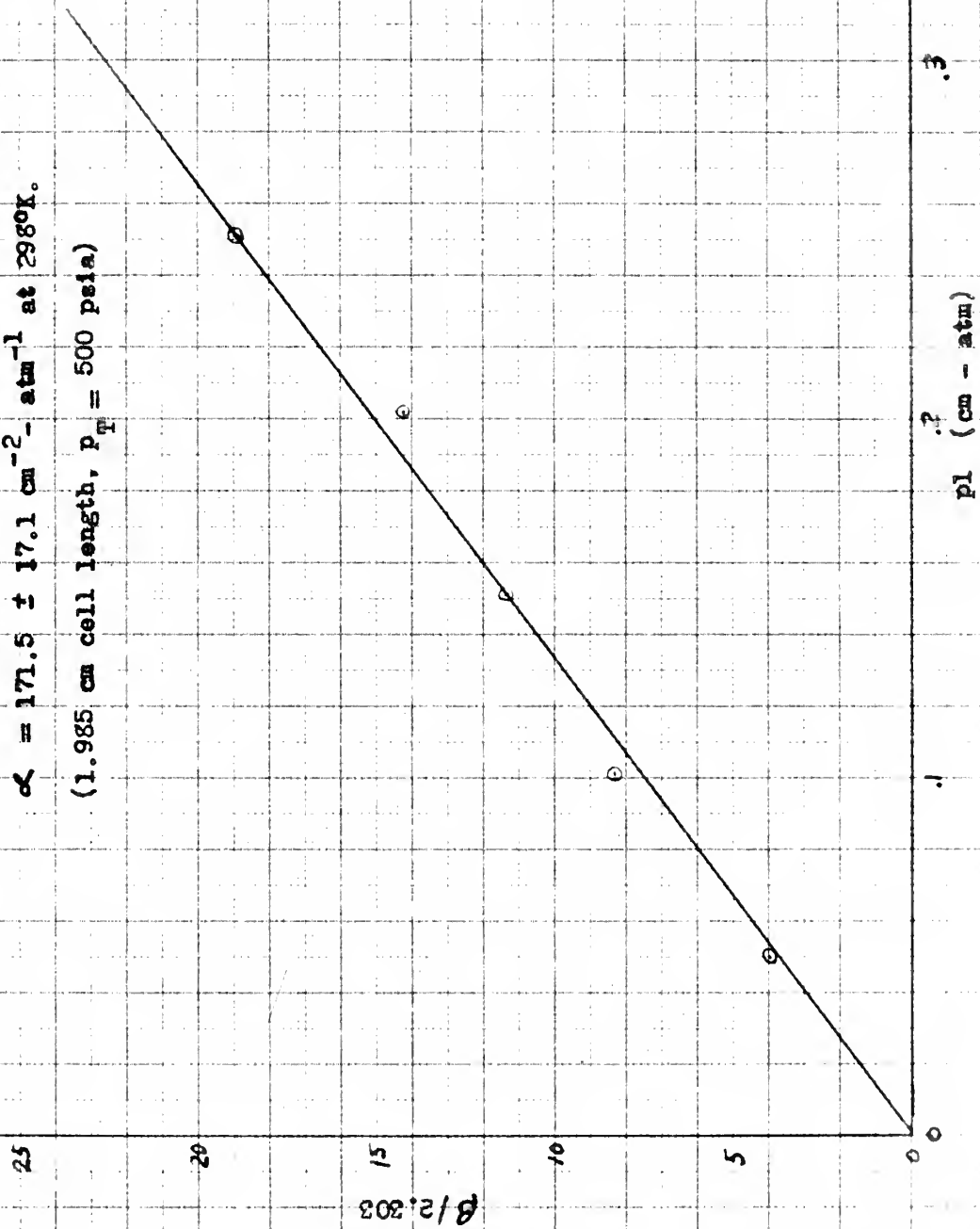


FIG. 11. Calibration curve for infrared spectrometer with

NaCl prism.

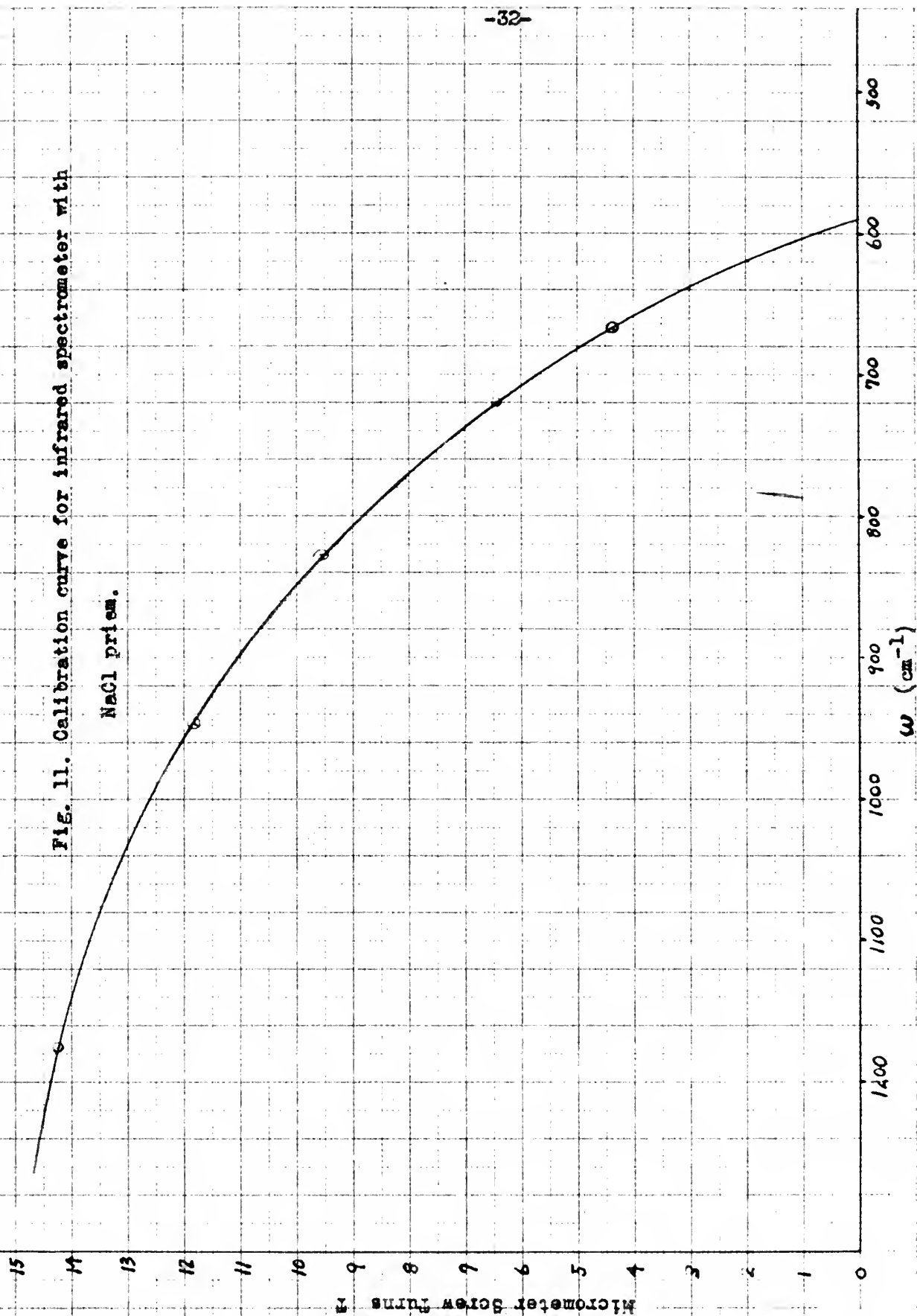
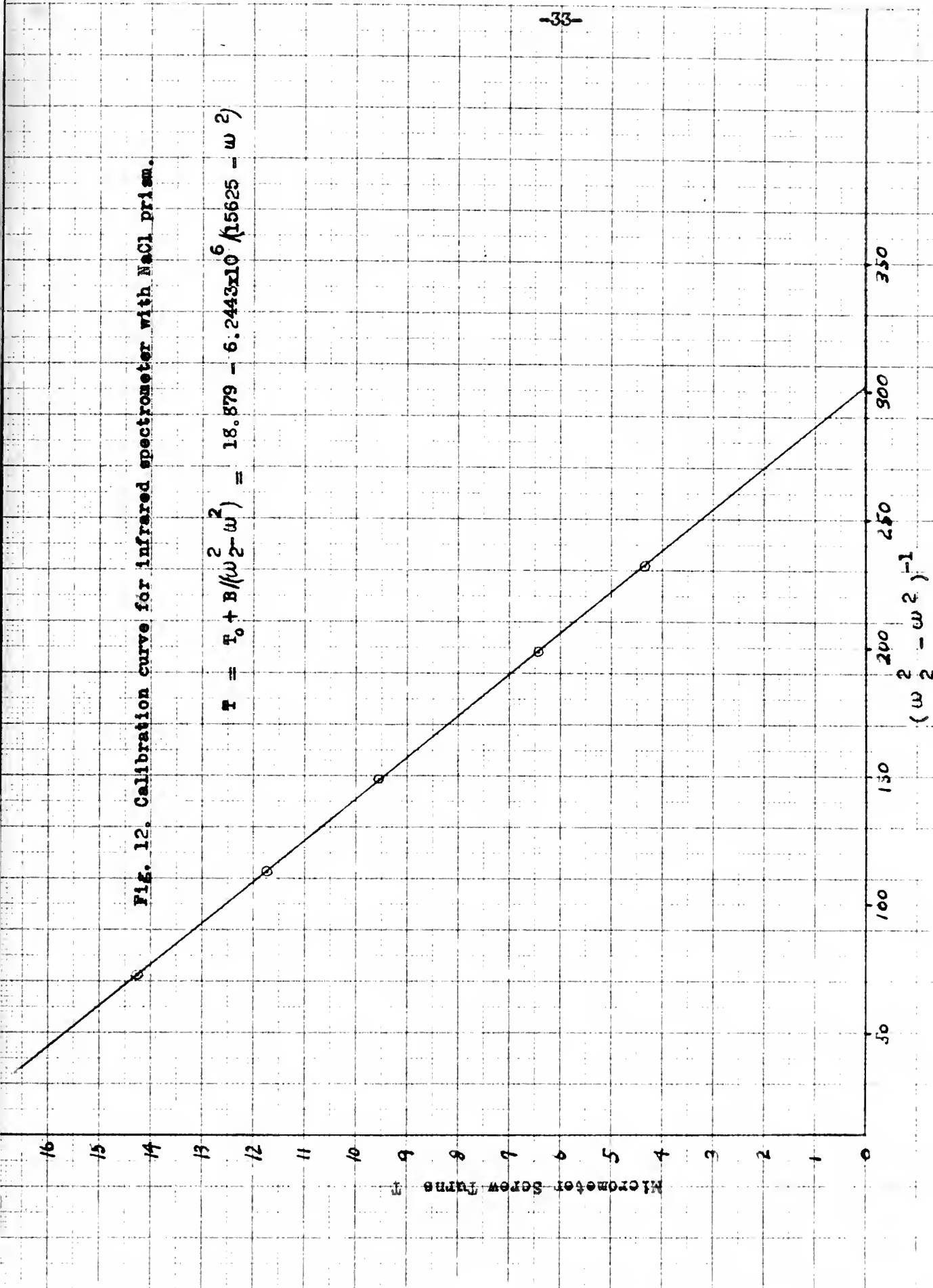


Fig. 12. Calibration curve for infrared spectrometer with NaCl prism.

$$T = T_0 + B(\omega_2^2 - \omega^2) = 18.879 - 6.2443 \times 10^{-6} (15625 - \omega^2)$$



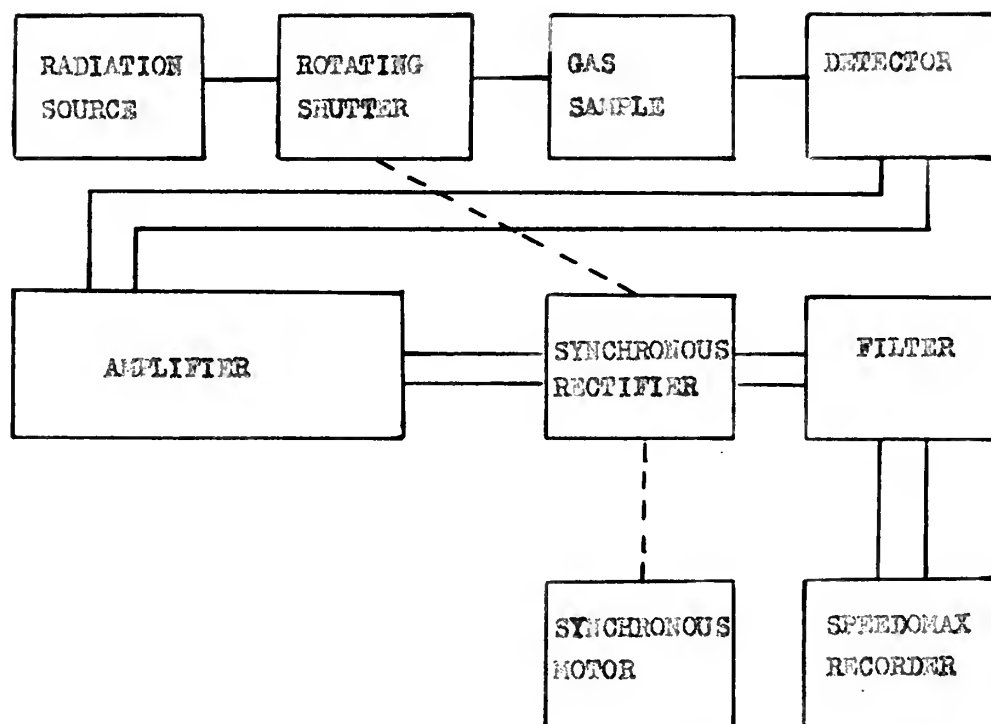


Figure 13. Block diagram of apparatus for measurement of total absorption of infrared radiation.

Fig. 14. Absorptivity α as a function of p_T for various fractional pressures of CO_2 at room temperature. (The CO_2 was pressurized with nitrogen).

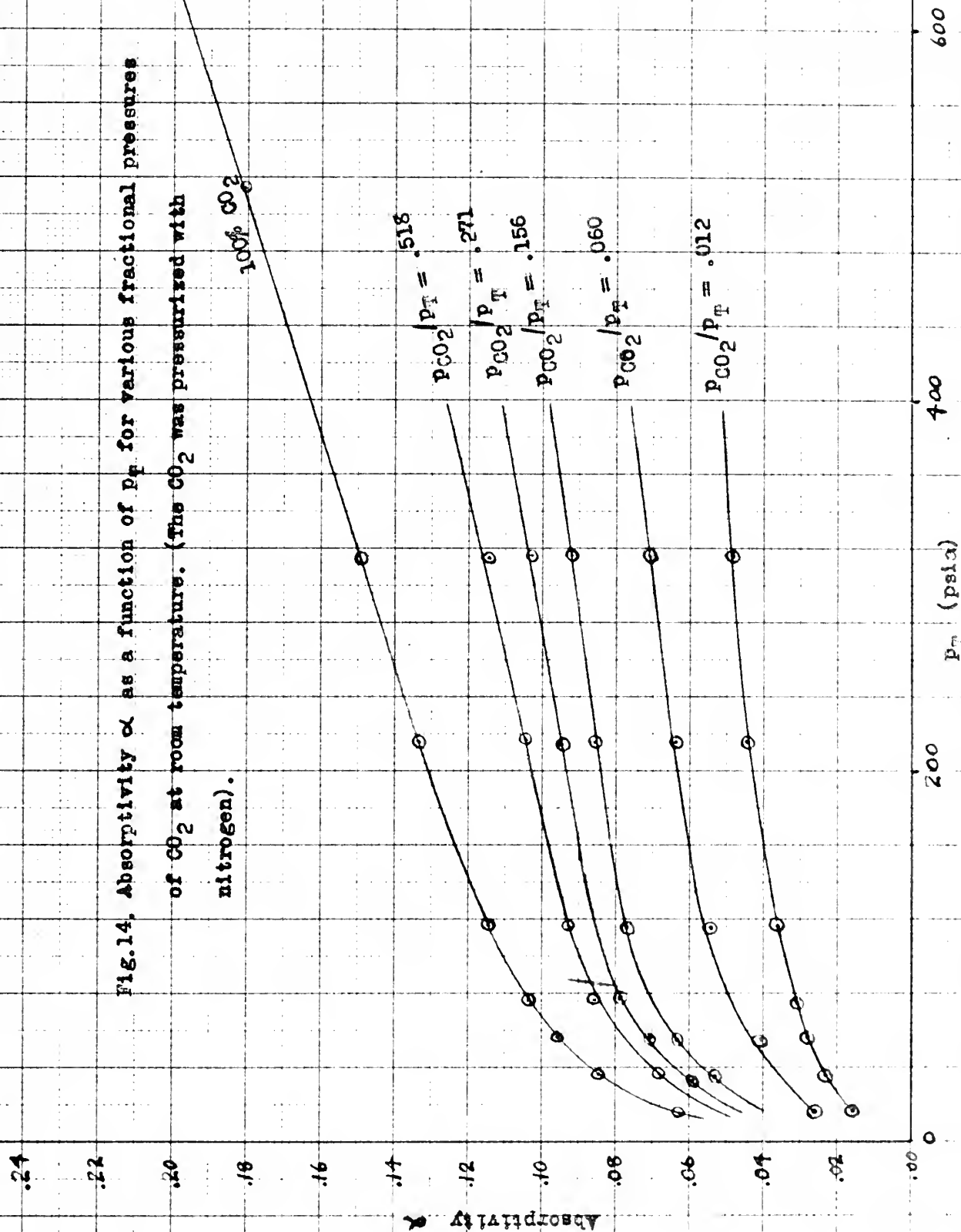


Fig. 15. Absorptivity α as a function of pl for CO_2 at room temperature and a total pressure of one atmosphere.

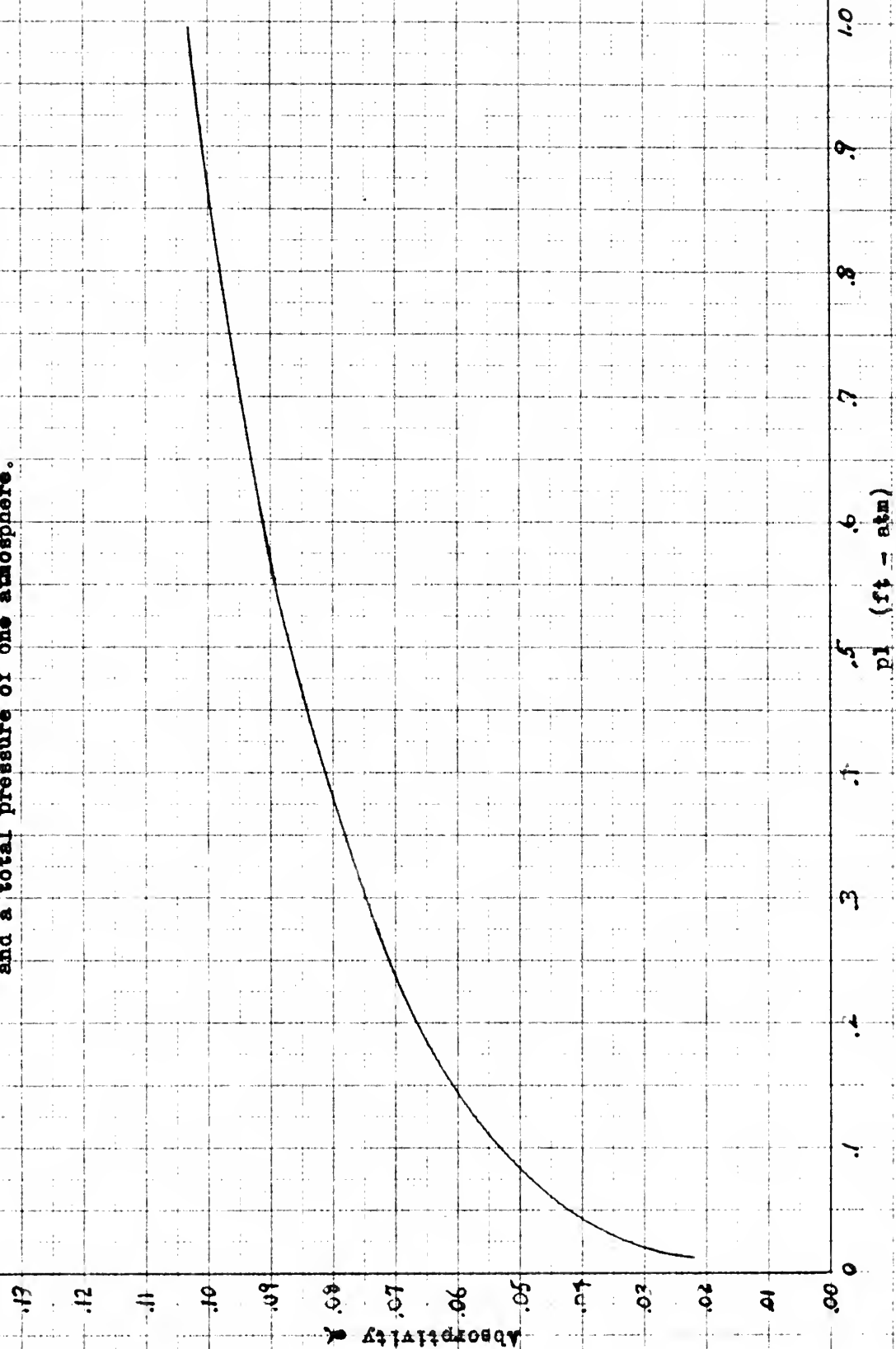


Fig. 16. Absorptivity α as a function of pl for CO_2 at room temperature and a total pressure of one atmosphere.

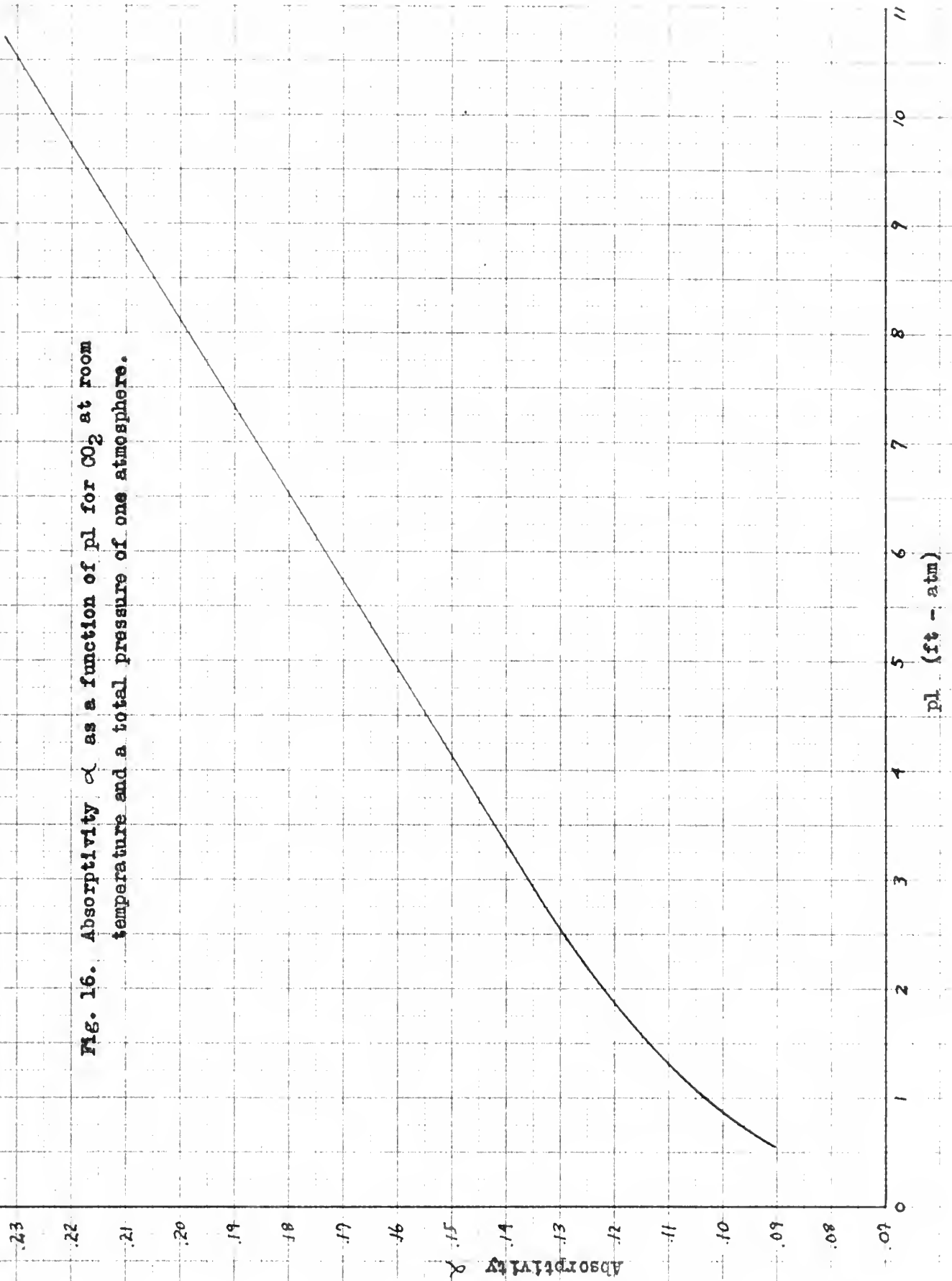


Fig. 17. Absorptivity α of CO_2 at room temperature as a function of
pl at various total pressures.

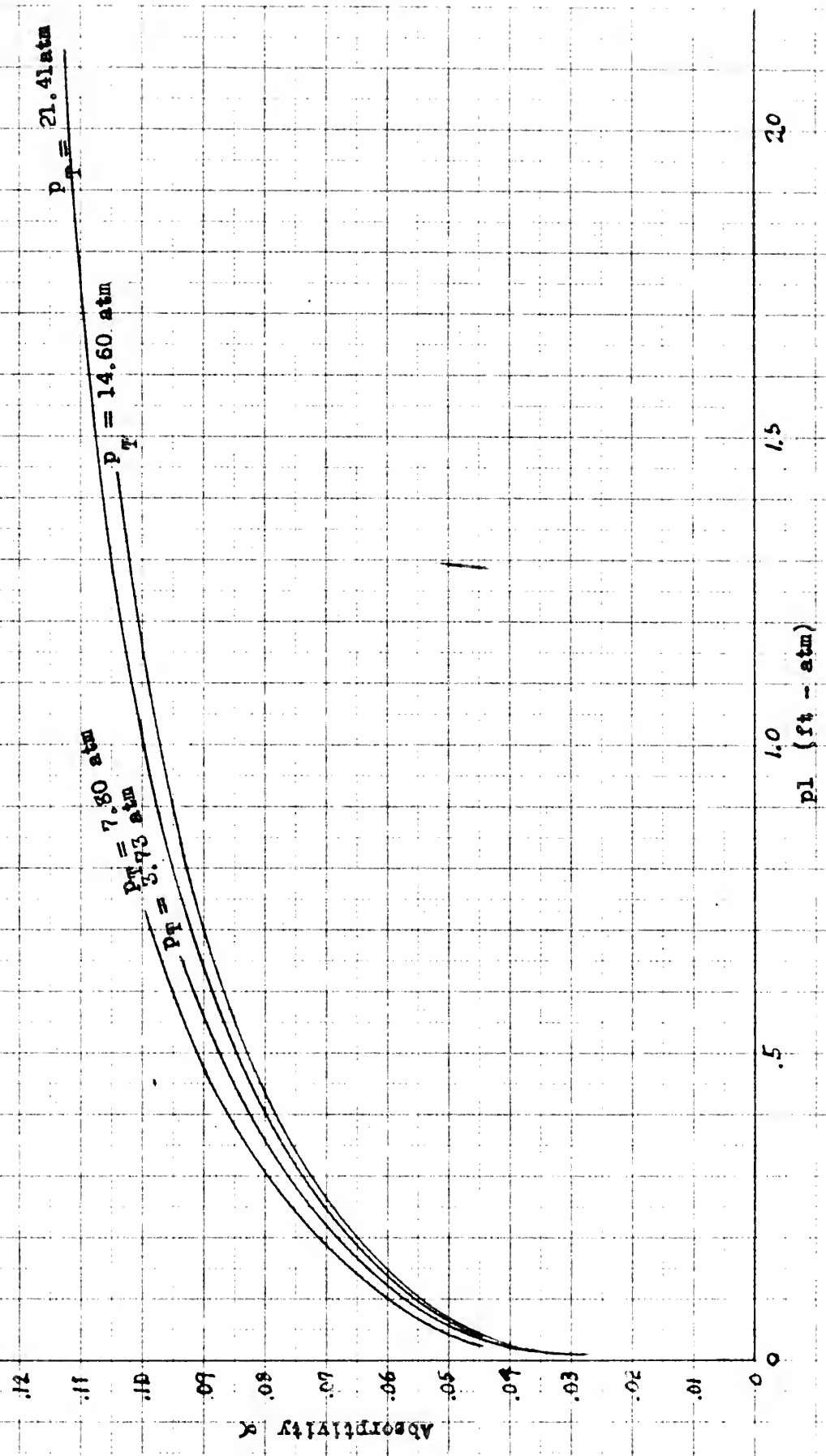


Fig. 18. Comparison of experimentally determined absorptivities as a function of optical density for CO_2 at atmospheric pressure and room temperature with the results of studies carried out by Hottel and Mangelsdorf.

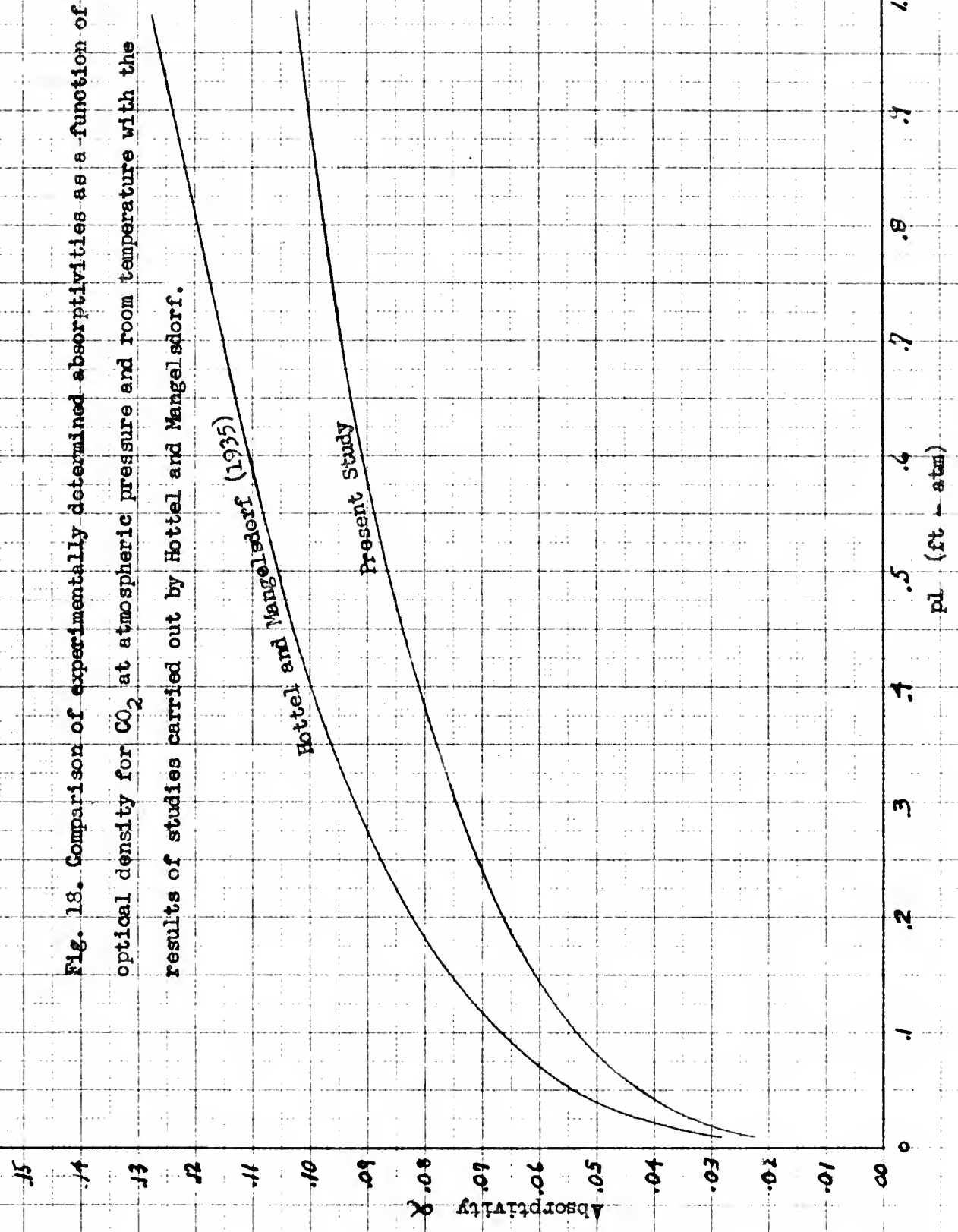
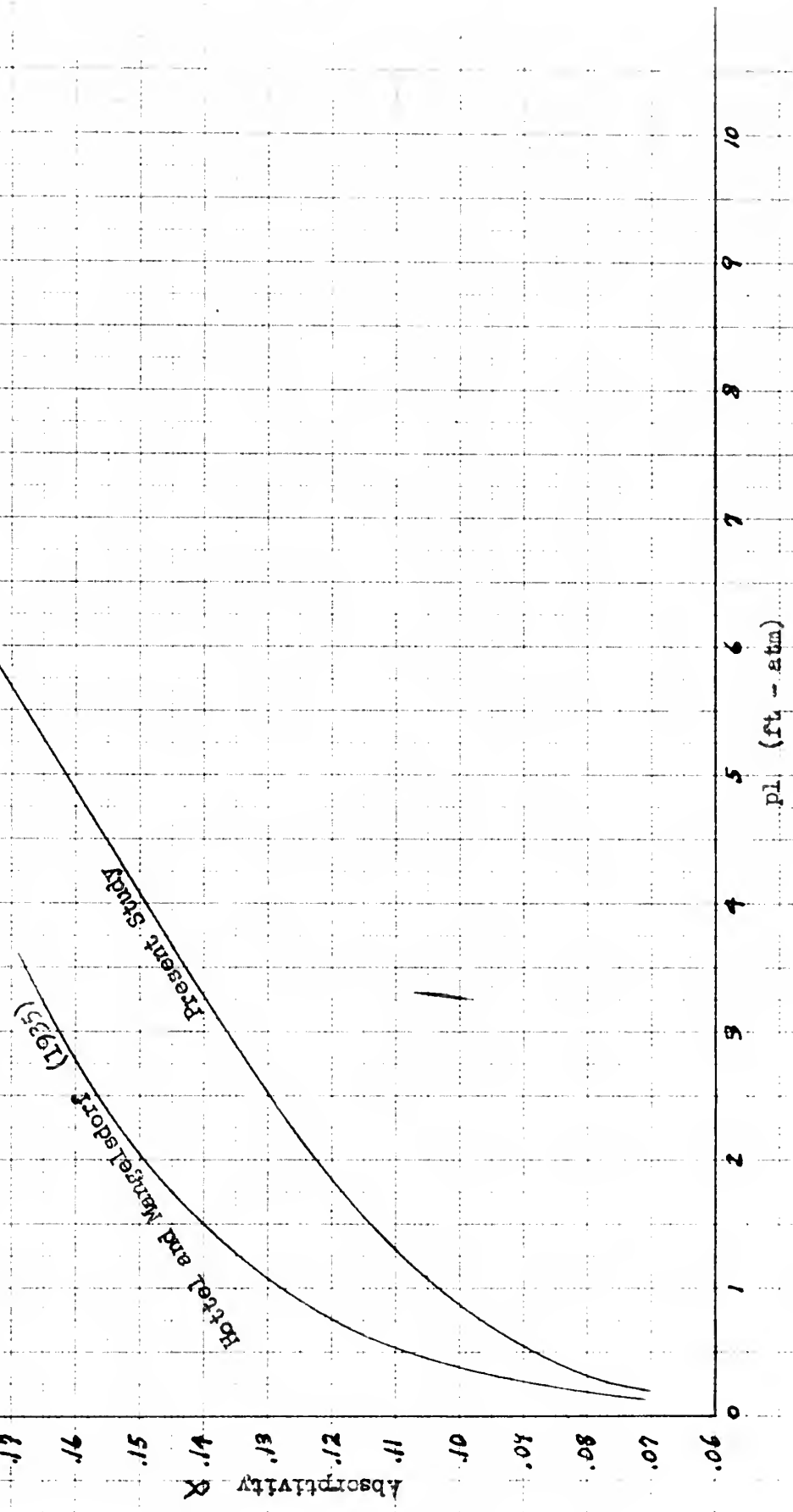


Fig. 19. Comparison of experimentally determined absorptivities as a function of optical density for CO₂ at atmospheric pressure and room temperature with the results of studies carried out by Hottel and Mangelsdorf.



OCT 2

BINDERY

18037

Thesis
H69

Holm

I. Integrated intensity
measurements of vibration-
rotation bands of carbon
dioxide. II. Total ...

OCT 2

BINDERY

18037

Thesis
H69

Holm

I. Integrated intensity
measurements for vibration-ro-
tation bands of carbon dioxide.
II. Total absorptivity measure-
ments on carbon dioxide at room
temperature.

Library

U. S. Naval Postgraduate School
Monterey, California

thesH69

I. Integrated intensity measurements for



3 2768 002 06927 0

DUDLEY KNOX LIBRARY